RSC Sustainability

ROYAL SOCIETY OF CHEMISTRY

PAPER

View Article Online
View Journal | View Issue

Check for updates

Cite this: *RSC Sustainability*, 2024, **2**, 2979

Sustainable agro-waste pellets as granular slow-release fertilizer carrier systems for ammonium sulfate†

B. G. K. Steiger, N. T. Bui, B. M. Babalola and L. D. Wilson *

In this study, several granular biocomposite carrier systems were prepared that contain biomaterials (chitosan, torrefied wheat straw and avian eggshells) as additive components at variable composition. The biocomposites were loaded with ammonium sulfate (AS) by two methods: (1) *in situ* addition of AS during pellet preparation, and (2) an adsorption method of AS after pellet preparation. Characterisation was carried out *via* spectroscopy (XRD, FT-IR) and complementary methods (TGA, acid stability). The pellet system (C1) by method (1) contained *ca.* 22 mg per g NH_4^+, whereas pellet systems by method (2) contained up to *ca.* 40 mg per g NH_4^+. The mol-ratio of $NH_4^+ : SO_4^{2-}$ varied from 2.18 (C1) to 2.72 (CW72), 2.97 (CW20), 2.64 (CW21) and 3.20 (CW22). Release studies in water showed that C1 pellets released almost 100% NH_4^+ within 3 h, while release varied from *ca.* 60% (CW72), *ca.* 40% (C20), 20% (C21) to 10% (CW22). By comparison, the systems prepared through method (2) showed a marginal increase of the release profiles up to 96 h. Granular AS carrier systems prepared by method (2) displayed greater mechanical stability and AS content *versus* the systems prepared by method (1). We demonstrated the ability to tailor the physico-chemical properties of such biocomposite carriers and highlight their promising potential as slow-release fertilizer systems.

Received 22nd March 2024
Accepted 19th August 2024

DOI: 10.1039/d4su00141a

rsc.li/rscsus

Open Access Article. Published on 27 August 2024. Downloaded on 2/20/2026 7:33:38 AM. This article is licensed under a Creative Commons Attribution-NonCommercial 3.0 Unported Licence.

Sustainability spotlight

Nitrogen use efficiency (NUE) in agricultural crop production is a key global issue due to fertilizer loss, where NUE values (<50%) are common, while slow release fertilizer (SRF) systems offer a promising solution. We highlight the development of ternary biocomposite carriers (TBCs) for ammonium sulfate (AS) that contain agro-waste biomass. We demonstrate an innovative and unique design of TBCs that reveal their potential as SRF systems for controlled-release of AS-fertilizer. As well, the TBC carriers are accessible *via* a facile synthetic strategy that is scalable and sustainable. The deployment of TBCs for SRF applications can address various UN Sustainable Development Goals: SDG-2 (no hunger), SDG-6 (water & sanitation), SDG-9 (industry, innovation & infrastructure), and SDG-12 (responsible consumption & production).

1 Introduction

In recent years, the emissions of greenhouse gases (GHG) through the ever growing agricultural sector has become increasingly scrutinized, where measures have been introduced to decrease GHG emissions.[1] In particular, GHGs (*e.g.*, CH_4, NO_x and CO_2) are common emissions from agricultural production, which contribute *ca.* 80% of anthropogenic N_2O emissions.[2] Additionally, another pertinent nitrogen source is the emission of ammonia (NH_3), with the agricultural sector that contributes to the release *ca.* 70% of the industrial emissions through fertilization activity.[3] Factoring in other anthropogenic activities such as livestock production, the release of ammonia can reach *ca.* 90% of the total emissions that are caused by human activities.[4] A concern of fertilizer application is the prevalent nitrogen (N) loss caused by bacterial activity, which can be *ca.* 40–70% of the introduced ammonia fertilizer depending on the method of application, soil topography and evaluation of the fertilization efficiency.[5,6] A common mitigation strategy to avoid such high losses and increase the fertilizer efficiency, whilst reducing the level of applied N-fertilizer, employs slow-release fertilizer (SRF) systems.

SRF systems aim to extend nutrient release within the soil profile whilst enhancing the nutrient availability. Different methods ranging from physical (*e.g.*, coating), chemically bound to physically combined in a compound form are available for SRF fabrication, while coating accounts for *ca.* 95% of the SRFs.[7] Evidently, urea formaldehyde is widely used as a SRF coating *via* polymerisation of urea, which displays a slower

Department of Chemistry, University of Saskatchewan, 110 Science Place – Room 156 Thorvaldson Building, Saskatoon, SK S7N 5C9, Canada. E-mail: lee.wilson@usask.ca

† Electronic supplementary information (ESI) available: Mould for granule preparation [(Fig. S1) TGA, DTG, IR, and XRD results for precursors and composites (Fig. S2–S6); ammonium sulfate release profiles (Fig. S7), and granule composite stability tests in aqueous media (Fig. S8)]. See DOI: https://doi.org/10.1039/d4su00141a

© 2024 The Author(s). Published by the Royal Society of Chemistry

Open Access Article. Published on 27 August 2024. Downloaded on 2/20/2026 7:33:38 AM. This article is licensed under a Creative Commons Attribution-NonCommercial 3.0 Unported Licence.

release compared to urea in its pristine form.[8] While coating has been deployed for decades (formaldehyde coated urea appeared in the 1950's, polyolefin and polyurethane in the 1970's and 1980's respectively), research into biopolymer coated SRFs witnessed the development of starch, chitosan, alginate, lignin *etc.* from the 1980's onwards.[9] Polymer-coated SRFs are notably state-of-the-art materials that employ synthetic polymers such as polyacrylamide, polyesters, polyethylene glycols, whereas polyurethane and polyethylene as common coating materials. Other synthetic polymers include polystyrene, polyether sulfone and polyvinyl alcohol. Besides polymers, inorganic materials (often encountered with organic modifiers) include gypsum, hydroxyapatite, zeolite, montmorillonite and bentonite have been used to formulate SRFs.[10] Loading ammonium nitrate into zeolites is a strategy to lower the rate of N-release due to changes in the diffusion profile of urea within porous zeolites.[11] Additionally, biochar and lignite have been associated with SRFs.[12] Further, materials such as (natural) rubber, (bio-)chars, cellulose, starch, chitosan *etc.*, alone or in combination with synthetic polymers or inorganic fillers can reduce the environmental impact of polymer-coatings.[13]

Specific examples of SRFs include polymer-coated fertilizer granules with polyvinyl alcohol (PVA) or carbonaceous materials (*e.g.*, biochar) with imbibed fertilizer.[14,15] Duan *et al.*[6] reported the fabrication of SRFs, their utility, and methodologies of these systems in detail.[6] In addition to the widely used method of chemically modifying urea, the application of synthetic polymers as coatings can result in deposition of synthetic polymer waste (up to 50 kg per ha per year) into the soil profile.[10,16] Further, removal of these coatings from soil is impractical and can result in considerable microplastic loading with potential detrimental effects.[17] Therefore, a suitable and affordable alternative to the currently employed common synthetic polymers (*e.g.*, polyurethanes, polyacrylamides) which are neither green nor sustainable are needed. The use of sustainable and green alternatives such as bio-based SRFs was outlined previously, where the benefits of biodegradable materials are manifold. However, there is a need to address the high cost and poor mechanical strength of natural polymers as SRF carriers.[6]

Previous work has outlined the utility of lignocellulose agro-waste materials for the design of biocomposites to yield adsorbents for ionic pollutant capture ranging from organic to inorganics (*e.g.* SO_4^{2-}, Pb(II), and cationic dyes).[18–20] A key feature of such biocomposites is the valorisation of common wastes such as (torrefied) wheat straw or oat hulls, without the need for complete pyrolysis into biochar, which reduces the energy input requirements to yield viable biocomposites for adsorption-based applications. In addition to (hemi-)cellulose and lignocellulose biomass waste, chitosan as β-(1 → 4)—linked glucosamine is generally derived from chitin, the second most abundant natural biopolymer. Chitin can be sourced from arthropods (*i.e.*, food waste such as crustaceans[21] where *ca.* 6 million tons are harvested per year), yeast or fungi.[22] Chitosan can serve as a binder that can provide active adsorption sites for cation binding.[23–25] Such types of biocomposites in their granular form that contain torrefied wheat straw at variable composition are known to have suitable mechanical properties for practical applications.[26]

To increase the valorisation potential of biogenic $CaCO_3$ obtained from avian eggshell (ES) waste, it is posited to function as a beneficial component to control soil acidity and porosity for such composites. ES application to soil helps to reduce blossom-end rot in plants like tomatoes and berries.[27] In addition, ES contains calcium, thus it has been effectively used as a low-cost liming source to improve the properties of acidic soils while it must be noted that application of ES to alkaline soils could be detrimental to plant growth.[28,29] Eggshell waste poses a significant disposal issue since the projected global egg production will reach *ca.* 100 million tons annually. In turn, this will ultimately contribute *ca.* 10 million tons of ES waste material.[30,31] The soil amendment benefits of ES waste has been reported, which can also improve the mechanical and chemical properties of soils,[32,33] along with the potential for retention of nutrients.[34,35] ES has been reported to improve the chemical and mechanical properties of composites. The addition of ES in the preparation of jute fiber mats was reported to give better tensile strength, flexural strength and impact strength to the mats, in comparison to composites without ES.[36] Further, a blend of corn starch and ES showed improvement in the spring index property.

Herein, an alternative strategy is proposed that involves the preparation of granular biocomposite carrier systems for a model ammonium sulfate (AS) fertilizer. Therefore, this study aims to investigate the development of a biocomposite carrier system by employing physical blends of chitosan, eggshell and torrefied wheat straw, in combination with ammonium sulfate (AS). The three constituents of the SRF offer environmental sustainability and biopolymer biodegradability. ES was incorporated as a negatively charged filler and to provide a more porous surface for the pellet systems, chitosan was used as a binder and to provide positively charged sites for anions. TWS was utilized as the main constituent in the pellets because the utilization of waste biomass is a cost effective and innovative way of solving major environmental challenges. Moreover, wheat is among the most cultivated crops worldwide, where torrefaction makes handling and grinding of wheat straw facile for composite preparation.

Herein, the potential utility of a matrix-based biocomposite granular carrier system for AS fertilizer is demonstrated. The granular carrier has potential utility for soil amendment, including unique SRF properties that obviate the need to employ synthetic polymer coatings. The SRF properties can be tailored according to the composition of the biomass components, which highlight the unique design and sustainability of this system. Although specialized studies are necessary to evaluate enhanced nitrogen use efficiency (NUE), the prepared AS-loaded biocomposite carrier systems (reported herein) can reduce fertilizer loss and GHG emissions upon further evaluation. This research addresses sustainable food production that aligns with the UN Sustainable Development Goals (UN SDGs).

2 Materials and methods

2.1. Materials

Chitosan (Ch; low molecular weight, DDA *ca.* 82%), KBr (FT-IR grade) and barium chloride anhydrous (99.9%+) were

© 2024 The Author(s). Published by the Royal Society of Chemistry

Open Access Article. Published on 27 August 2024. Downloaded on 2/20/2026 7:33:38 AM. This article is licensed under a Creative Commons Attribution-NonCommercial 3.0 Unported Licence.

purchased from Sigma-Aldrich (Oakville, Canada). Glacial acetic acid (99.7%), sodium chloride (ACS), sodium sulfate anhydrous (ACS), glycerol, isopropanol, hydrochloric acid (37%), ammonium sulfate (ACS) and sodium hydroxide (ACS) were obtained from Fisher Scientific (Ottawa, Canada) while ninhydrin (reagent grade) was purchased from Ward's Science (Mississauga, Ontario, Canada). The torrefied wheat straw (TWS; 220 °C) was received from the torrefaction facility within the College of Engineering at the University of Saskatchewan. Eggshells were collected from a local source and washed extensively with tap water, followed by thorough rinsing with distilled water and with Millipore water. The ES waste was dried in an oven at 105 °C for 24 h. The dried ES material was ground and sieved with size No 40 (425 micrometre) of U.S.A. Standard Testing Sieve to obtain the ES powder (ESP) for use herein. Millipore water with a resistivity of 18.2 M Ohm cm was used throughout, unless otherwise stated.

2.2. Preparation of the pellets

The preparation of the granular pellets with the following components: ES, powdered TWS and chitosan at variable composition (with or without AS) were mixed in their dry state before adding acetic acid aqueous solution as a dispersion additive (see Table 1 for their respective particle size estimation).

The components were added according to the following procedure (*cf.* Scheme 1): 10 g batches of variable composition were mixed by weight, and 0.2 M acetic acid (*ca.* 10–25 mL) was added for uniform dispersion consistency across all systems. The mixture was quickly mixed to yield a paste that was pressed into moulds (SPP Trays; S&B, Vlašim, Czech Republic; *cf.* Fig. S1 in the ESI†), and dried overnight at *ca.* 22 °C.

For method 1 (*in situ* N-carrier system, *cf.* Table 2 for the respective wt%) TWS and ES were combined with AS and Ch depending on the intended AS content. The components were mixed in a mortar and *ca.* 10–12 mL of 0.2 M acetic acid added, mixed to a paste, and pressed into the mould (*cf.* Scheme 1 and Table 2). After drying at *ca.* 22 °C for 1–3 days, the pellets were removed from the mould.

For method 2, only Ch, ES, and TWS were mixed in their powdered form, combined with acetic acid, and then mixed into a paste (*cf.* Table 3 for the composition). The paste was pressed into the mould to form cylindrical pellets. The final pellets were dried for 1–3 d at *ca.* 22 °C, and then removed from the mould. The pellets (10 g) were neutralized overnight at 22 °C in 250 mL 0.5 M NaOH solution. Then, the pellets were rinsed until pH 7 was attained. Subsequently, 1 g of the neutralised pellets were immersed in 1 M AS solution (100 mL) for 18–24 h at 22 °C. Then, the imbibed pellets were removed, rinsed to remove excess AS solution and dried.

The size of the pellets CW1, CW72, CW20–22 are shown in Table S1 of the ESI.†

Table 1 Particle size range estimation of the powdered constituents for the preparation of the N-carrier systems in pellet form in wt%

Particle size range (μm)	Chitosan (μm)	Eggshell (μm)	TWS (μm)
>425 < 150		87	65–67
>125 < 75	100	12	33–35
>75		1	

Scheme 1 Schematic representation of blending the powdered constituents into a moulded paste, where the resulting pellets were obtained upon drying. Note that method 1 incorporates ammonium sulfate (AS) during the pellet preparation, whereas method 2 involves incorporation of AS after pellet preparation *via* imbibing pellets in an adsorption process. The black square is the mold for the pelet preparation.

2.3. Spectrophotometric determination of the ammonium and sulfate concentration

2.3.1. Ammonium concentration determination. Aliquots of diluted ammonium solution were added to 0.25 mL 0.128 M NaOH with 0.04 M ninhydrin solution (1 mL).[37] A stable colour was developed after *ca.* 45–60 min and measured *via* UV-vis (Thermo Fisher Scientific Spectronic 200E) spectrophotometry at a fixed wavelength (508 nm).

2.3.2. Sulfate concentration determination. To determine the sulfate concentration, the turbidity method outlined by IS 3025 (Part 24) was employed.[38] Briefly, a 25 mL total volume was used, where 1.25 mL of conditioning reagent was added with an appropriate sample aliquot of AS. Approximately 100 mg barium chloride was added to each sample, and then shaken. Samples were analysed after 10 minutes *via* UV-vis spectrophotometry at 420 nm, as described in Section 2.3.1.

2.4. Characterization

2.4.1. Stability of pellet systems at different pH. A qualitative and preliminary evaluation of the pellet systems in solutions at different pH values was achieved by employing two

Table 2 Pellet compositions for materials prepared according to method 1

Method 1							
Additive wt (g)	Composite systems						
	C1	C2	C3	C4	C5	C6	C7
TWS	5	5	5	2	4	6	8
AS	1	2	3	6	4	2	1
ES	1	1	1	1	1	1	0.5
Ch	3	2	1	1	1	1	0.5

Open Access Article. Published on 27 August 2024. Downloaded on 2/20/2026 7:33:38 AM. This article is licensed under a Creative Commons Attribution-NonCommercial 3.0 Unported Licence.

Table 3 Pellet composition for materials prepared according to method 2

Method 2				
Additive wt (g)	Composite systems			
	CW72	CW20	CW21	CW22
TWS	8	6	4	2
ES	1	2	3	4
Ch	1	2	3	4

solutions with different pH. Acetic acid solutions at pH 5 adjusted with $NaOH_{(aq.)}$ and solution of $HCl_{(aq.)}$ at pH 1.85. In this step, 1–2 pellets were transferred to 8-dram vials and approximately 10 mL of either solution added to each vial. The vials were left over night at 22 °C and inspected visually for mechanical instability (*i.e.* crumbling or breakage).

2.4.2. FT-IR spectroscopy. Samples were prepared by co-grinding (pestle/mortar) KBr and sample (10 : 1 ratio), where the spectra were recorded on a Bio-Rad FTS-40 (Bio-Rad Laboratories Inc., USA) at 295 K. A spectral range of 400–4000 cm^{-1} with resolution of 4 cm^{-1}. A minimum of 64 scans were collected and a spectral background was obtained against pure KBr. The spectra were normalized.

2.4.3. Thermogravimetric analysis (TGA). The decomposition profiles were obtained by employing a Q50 TA Instruments TG Analyzer (TA Instruments, USA) under an inert gas atmosphere (N_2). The samples were placed in an open aluminum pan, and exposed to 1 min equilibration at 30 °C, before exposure to a heating rate of 10°min^{-1} until 500 °C. TG curves were normalized, DTG curves were plotted as weight loss *vs.* temperature.

2.4.4. (Powder) X-ray diffraction (XRD). A Bruker-D8 Advance Powder (Billerica, USA) XRD instrument was used to analyse the composites. A CuKα radiation (40 kV and 30 mA) with $\lambda = 1970.2$ nm at a 2θ angle range from 5° to 90° was used to obtain the XRD profiles.

2.4.5. Ammonium sulfate content. The AS content of the pellets was determined by immersing *ca.* 1 g pellets in 5 M NaCl solution (0.1 L) overnight while agitating at *ca.* 20 °C to destabilize the pellet matrix. After separation of the (mostly powdered) suspended constituents, the supernatant was analysed for ammonium and sulfate concentration, as described in Section 2.3 of this work.[39]

2.4.6. Release studies. To obtain the AS release profiles, the respective pellets (*ca.* 1 g) were added to millipore water (50 mL) and semi-dynamic release profiles were studied over 96 h. This involves the removal of 10 mL aliquots and replacing with 10 mL millipore water at specific time intervals.[39]

2.4.7. Statistical analysis. A statistical analysis was performed with Statgraphics Centurion XV and one-way ANOVA analysis with 95% confidence level ($p = 0.05$) according to Fisher's test, where two measurements were employed.

3 Results and discussion

Herein, the first stage of evaluation of the composites was performed through tactile and visual testing prior to selection of suitable biocomposites as stable pellet systems at variable composition for further study. The physico-chemical characterization and subsequent testing of ammonium sulfate loading occurred *via* two strategies: (1) *in situ* incorporation of AS during pellet preparation, and (2) incorporation of AS *via* an adsorption process after pellet preparation (*cf.* Scheme 1). To assess the potential utility of the various granular biocomposites as SRF carrier systems, a study of the fertilizer release profiles over time was monitored in aqueous media under semi-dynamic conditions.

3.1. Composite selection for further evaluation

The investigated composites can be divided into two categories, based on the mode of AS addition: method 1 and method 2. Table 4 shows the composition of pellets prepared according to method 1, in addition to the relative tactile stability results.

Based on the results in Table 4, only one composite displayed the necessary tactile and handling stability to undergo further study (*i.e.*, no crumbling), while all other composites were brittle under applied pressure. The incorporation of ionic compounds (ammonium sulfate) appear to diminish the cohesion and mechanical stability among the constituent additives incorporated within the pelletized biocomposite. Thus, the C1 system obtained *via* method 1 was the sole composite chosen for further investigation.

Based on previous studies that reveal favourable cohesion and mechanical properties of TWS-containing pellets, the following compositions prepared *via* method 2 were chosen for AS imbibing, as listed in Table 5.

In contrast to the composites shown in Table 4, these composites displayed notably greater tactile strength without immediate crumbling during handling. Therefore, all four systems were further investigated as potential SRF carrier systems.

3.2. Characterisation

3.2.1. Stability of pellet systems at different pH. To briefly and qualitatively evaluate whether the prepared pellets withstand acidic conditions, solutions with pH 5 and pH 1.85 were employed to compare with other types of composites reported

Table 4 Composition of the AS-containing composites with C1–3 having a fixed TWS content, while composites C4–7 have variable TWS content to allow investigation of increased AS loading and tactile mechanical stability (nil or low to high) upon drying

Method 1							
	Fixed TWS			Variable TWS			
Additive wt (g)	C1	C2	C3	C4	C5	C6	C7
TWS	5	5	5	2	4	6	8
AS	1	2	3	6	4	2	1
ES	1	1	1	1	1	1	0.5
Ch	3	2	1	1	1	1	0.5
Stability	High	Low	Low	Medium	Low	Low	Nil

© 2024 The Author(s). Published by the Royal Society of Chemistry

Open Access Article. Published on 27 August 2024. Downloaded on 2/20/2026 7:33:38 AM. This article is licensed under a Creative Commons Attribution-NonCommercial 3.0 Unported Licence.

Table 5 Composition of the four selected non-AS containing pelletized composites for further imbibing with AS in solution and mechanical stability after drying

Method 2				
Additive wt (g)	CW72	CW20	CW21	CW22
TWS	8	6	4	2
ES	1	2	3	4
Ch	1	2	3	4
Stability	High	High	High	High

in an independent study, where the samples were prepared with kaolinite instead of eggshells (*cf.* Table 6).[19]

The qualitative and visual analysis of the mechanical stability in solution (*cf.* Fig. S9; ESI†) showed that all composites are stable at pH 5, whereas CW20–22 display structural instability in aqueous media at pH 1.85.

3.2.2. FT-IR. IR spectroscopy enables the study of interactions among respective components, which depend on an increase or decrease of the observed IR signature bands (*cf.* Fig. 1).

When comparing the IR spectra of the raw materials (*cf.* Fig. S5 in ESI†) with the prepared composites, specific spectral bands were retained that correspond to the ratios of the raw materials of the composites (especially for ES). Herein, ES show characteristic peaks at 715 cm^{-1}, 875 cm^{-1}, 1427 cm^{-1} (largest band) and a specific smaller band at 1801 cm^{-1} that shows no evident overlap within the composites.[40] All raw materials show contributions between 3600–3000 cm^{-1} (OH– and NH– groups) and C–H peaks around 2900 cm^{-1}. In the case of ES, this was explained by the presence of minor organic impurities left after membrane removal and residual moisture. TWS shows a peak at 1740 cm^{-1} that was assigned to carboxylic acid (C=O stretching), while chitosan observes an amide stretching band at 1673 cm^{-1}, which is absent in TWS, where it is observed for the composites. The C–O–C bands for the biopolymer backbone was observed near 1165 cm^{-1} and potential contributions from the ES fraction. The band at 1600 cm^{-1} attributed to C=C stretching is retained in TWS that is observed for all composites. In general, it was postulated that the composites are physical blends, where the composition reflects the approximate content (%) of the raw materials incorporated during preparation (Fig. 1).

3.2.3. TGA. Thermogravimetric decomposition profiles not only allow to infer the compositional variation within the materials, but also the role of interactions among components that influence the physico-chemical properties of the materials,

Table 6 Visual observation of mechanical stability (breaking *vs.* non-breaking) in solution at pH 5 and pH 1.85

	C1	CW72	CW20	CW21	CW22
pH 5	✓	✓	✓	✓	✓
pH 1.85	✓	✓	✗	✗	✗

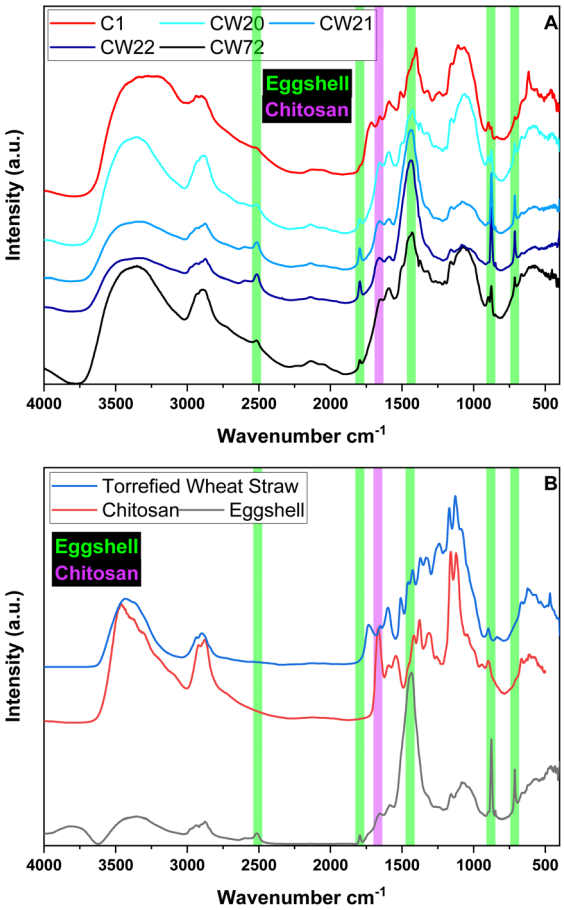

Fig. 1 FT-IR spectra (normalised) of five types of composites (A) and their respective raw materials (B) with characteristic bands highlighted to support the presence of intact eggshells after composite formation.

according to peak shifts in the TG profile. To better identify where the TG events occur, DTG profiles (derivative weight loss in °C min^{-1}) are diagnostic for highlighting temperature values

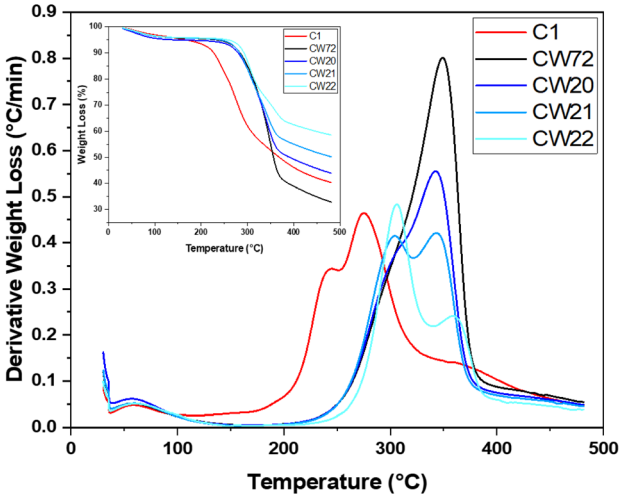

Fig. 2 DTG profiles of the prepared and for further investigation selected composites (with TG curves as the inset).

Open Access Article. Published on 27 August 2024. Downloaded on 2/20/2026 7:33:38 AM. This article is licensed under a Creative Commons Attribution-NonCommercial 3.0 Unported Licence.

and magnitude of weight loss, whereas the TG profiles (TG wt loss in %) can identify the amount of lost water and other information such as the residual weight *etc.* (*cf.* Fig. 2).

The raw materials in case of chitosan (*cf.* Fig. S3 in the ESI†) show a rather narrow thermal event near 300 °C, whereas TWS has a broader band that overlaps with a smaller band near 300 °C that indicates hemicellulose for the cellulosic constituents near 350 °C.[41] Calcium carbonate was used as a control for the eggshell materials to estimate the influence of the washing procedure on the residual organic components. It was assumed that *ca.* 2 wt% organic content was retained by the washed eggshells used for pellet preparation, which overlap at 300 °C, as noted in the TG profiles. Ammonium sulfate (both industrial and ACS grade) show nearly identical decomposition profiles, indicating only minor amounts of impurities are present and complete decomposition occurs near 500 °C. The thermal events (onset *ca.* 287 °C for the ACS grade ammonium sulfate) are clearly evident prior to the major TG event at 393 °C, where the mechanism for the thermal event is detailed elsewhere.[42,43] The C1 sample shows two distinctive peaks at 244 °C (*cf.* Fig. S4, ESI†) that are shifted to an earlier onset, attributed to interactions between AS and the constituent additives. Continued decomposition and a potential peak around 360–370 °C is shifted to a higher temperature value, as compared with TWS. CW72 reveals a shoulder near 300 °C and a prominent TG event near 350 °C that resides close to TWS, due to its high TWS content. The composites CW20 and 21 show a larger thermal event near 305 °C, which relates to the greater chitosan content *versus* CW72. CW20 and CW21 show a DTG profile that concurs with cellulose at 342 °C, while CW22 has this thermal event shifted to 361 °C.

3.2.4. PXRD. X-Ray diffraction (XRD) is a valuable tool to identify crystallinity within a material, along with detection of crystalline structural features of ES upon formation of the pelletized composite (*cf.* Fig. 3).

In comparison with the raw materials (*cf.* Fig. S6, ESI†), the XRD bands (16° and 22°) that appear for TWS are broad for all composites with variable intensity, according to the relative TWS content. Chitosan reveals a broad XRD band near 20°, which overlaps with the TWS bands for all composites. With reference to ammonium sulfate, the industrial AS sample shows additional bands that occur due to undefined mineral impurities. However, the XRD bands cannot be assigned to the composite (due to the relatively low concentration and overlap of the strongest band at 23° with TWS). On the contrary, the expected signals for eggshells (mainly 29.6°, 36.2°, 39.6°, 43.4°, 47.8° and 48.8°) were observed and remain unchanged, indicating that no apparent phase change occurs.[44,45] The XRD line intensity appears to vary with changes in the relative concentration of the additive components, as expected.

3.2.5. Ammonium sulfate content. As outlined in Section 2.4.5., the pellets were subjected to saline conditions to undergo ion exchange with sodium and chloride ions, without altering the pH dependent analytical method for NH_4^+ determination *via* ninhydrin. C1 was expected to have 10% AS content as a baseline (a total 27 mg ammonium and 73 mg sulfate per 1 g pellet; based on its weight content from AS). The determined values are listed in Table 7.

Herein, the pellet system prepared with 10% AS content that was added to the mixture for C1 was estimated to contain 22.44 mg ammonium (83% of the expected value) and *ca.* 55 mg sulfate (75% of the expected value). This trend may indicate matrix effects that may contribute to the results, based on the high NaCl concentration employed. However, the obtained values provide a sufficient comparison of the available AS content within the different pellet matrices. The ammonium to sulfate ratio (on a molar basis) was expected to be 2, based on the stoichiometric ratio for the salt ($(NH_4)_2SO_4$) system, which was similarly noted for C1. All other pellet systems showed both higher ammonium content (up to 40 mg for CW72 and CW21) with less available sulfate in solution (ratios closer to 3, in agreement with the lower release profile for sulfate (*cf.* Fig. S7†) that indicates a stoichiometric excess of ammonium occur in solution *versus* sulfate). This can be due to the adsorption capacity of the pellet systems favouring release of the ammonium cation above the 2 : 1 stoichiometric ratio. This is understood due to the likelihood of ion exchange of sulfate with acetate anions, according to the Hofmeister effect since sulfate preferentially associate (*versus* acetate) with the protonated amino sites of chitosan to form salt bridges. The preferential association of acetate over chloride was revealed in a study of the phosphate flocculation properties of chitosan with variable counterions (chloride *vs.* acetate).[34]

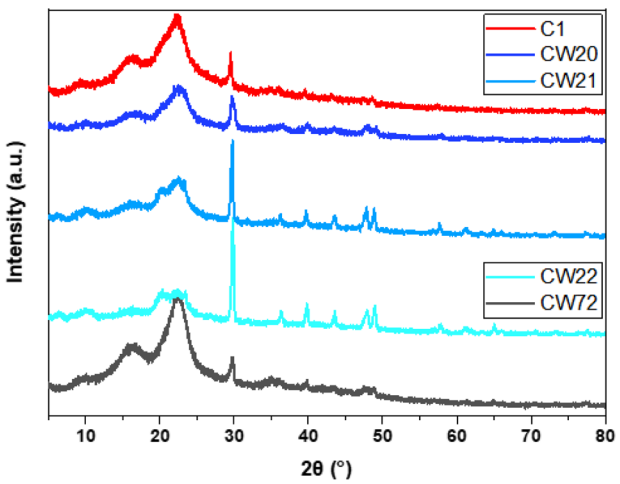

Fig. 3 PXRD profiles of various pellet systems.

Table 7 Granular composites with ammonium and sulfate incorporation and estimation of AS content *via* desorption profiles in 5 M $NaCl_{(aq.)}$ solution

	C1	CW72	CW20	CW21	CW22
NH_4^+ (mg)	22.44	39.31	33.02	40.43	33.47
SO_4^{2-} (mg)	54.79	77.20	59.27	81.69	55.79
AS (mg)	77.23	116.51	92.29	122.11	89.25
NH_4^+/SO_4^{2-}(mol-ratio)	2.18	2.72	2.97	2.64	3.20

© 2024 The Author(s). Published by the Royal Society of Chemistry

Open Access Article. Published on 27 August 2024. Downloaded on 2/20/2026 7:33:38 AM. This article is licensed under a Creative Commons Attribution-NonCommercial 3.0 Unported Licence.

However, it is evident that imbibing pellet systems in a 2-step process yields mechanically more stable pellets with higher loadings of AS such as CW72 that has 75% higher AS content than C1 with 10% AS content during preparation.

3.2.6. Release studies. In the context of potential carriers for SRF-based applications, a comparison of the release profiles for the AS-containing composites in water was undertaken (*cf.* Fig. 4). A comparison of various composites enables the evaluation of variable release profiles, according to the relative composition of these systems.

4.2.6.1 NH_4^+ release. The initial release of ammonium across all composites occurred within 3 h, with *ca.* 50% of the total released ammonium in the first 0.5 h. The composite produced *via* method 1 *versus* pellet systems prepared *via* method 2, revealed a near complete release of ammonium over this time frame. A slow-release process for composites prepared *via* method 2 occurred between 3 h and 96 h.

4.2.6.2 SO_4^{2-} release. In contrast to the ammonium release profiles, the first 3 h showed less than 60% of the total sulfate released. After 3 h, no evidence of a slow-release profile was observed for any of the composites. In turn, a steady release up to 96 h was noted, which indicates limited control over the sulfate release *versus* ammonium, irrespective of the method of preparation. Future studies are required to provide an equal sulfate retention and release profile to increase the suitability of these systems for SRF application of AS.

The uniform release of AS over a longer time interval is preferred to facilitate adequate nutrient release profiles. Thus, specific studies are required to assess the NUE of SRFs in a realistic manner.[46] Herein, the release profiles in water were determined to highlight differences between materials made *via* method 1 and method 2. The results herein provide a comparison of AS release among various composites on a relative scale to enable screening of suitable carrier systems reported herein.

This can be further highlighted by a comparison of the sulfate release for the ratio of released ammonium and sulfate (*cf.* Fig. S7 in ESI†). The C1 system released 4× the wt content of ammonium over sulfate in the first 3 h, indicating the comparatively slow initial sulfate release. By comparison, the other composites ranged between 2–3× ammonium released over sulfate. In contrast to the gradual ammonium release suitable for SRF applications, the sulfate release is comparatively rapid and resides between 60–100% for all composites within 96 h. The decreased initial ammonium release corresponds to an increased chitosan content in the granular matrix facilitating a lower initial release in conjunction with a gradual ammonium release thereafter.

3.2.7. Statistical analysis of NH_4^+ release. Based on the aforementioned lack of controllability for the release of sulfate, as compared with ammonium release, only the NH_4^+ release was investigated *via* statistical analysis.

To establish whether or not the data points shown in Fig. 4A are statistically significantly different from each other, a multifactorial analysis of variance (ANOVA) and Fisher's least significant difference (LSD) methods were performed.[47,48] Herein, time and SRF systems are the main factors, where significance values of less than 0.05 (95% confidence interval) were reached (*cf.* Tables S2, ESI†). Thus, it can be implied that time has a significant statistical effect on the ammonium release.

To investigate the ammonium release for the investigated SRF systems, both ANOVA and Fisher's test were performed (*cf.* Table 8 as example for the time at 3 h that describes two cases and Tables S2 and S3† for the multi-factorial analysis parameters and ANOVA statistical results for all three times).

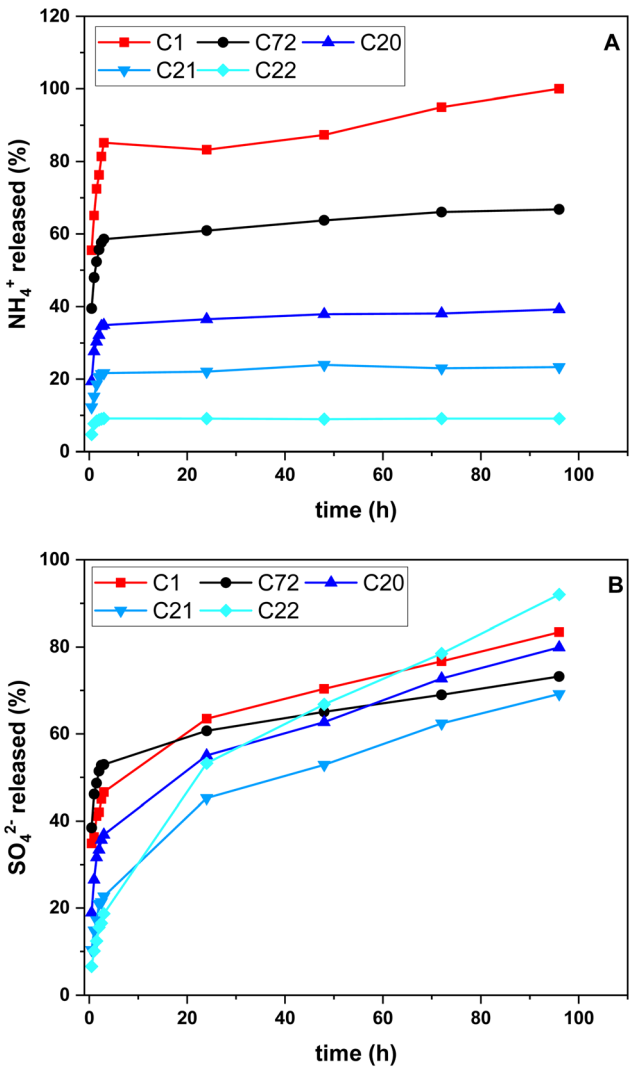

Fig. 4 Release profiles for all pellet systems: (A) in ammonium (%) and (B) in sulfate (%) for variable time.

Table 8 Statistical analysis (p = 0.05) of LSD (Fisher's test) of the release of all pellet systems after 3 h where A to E denote statistically signficant groups based on homogenous groups

Pellets	Cases	Mean	Homogeneous groups
CW22	2	0.09075	A
CW21	2	0.220785	B
CW20	2	0.365225	C
CW72	2	0.60914	D
C1	2	0.96348	E

Open Access Article. Published on 27 August 2024. Downloaded on 2/20/2026 7:33:38 AM. This article is licensed under a Creative Commons Attribution-NonCommercial 3.0 Unported Licence.

The number of homogeneous groups (5, A–E) indicate that all composites are statistically significantly different from each other. Herein, the ANOVA test indicates a significant result for one factor, this indicates that for that factor, there is at least one group (data point) that differs from the other. Further, the LSD was compared to the calculated means and a difference is declared when the calculated mean value exceeds the LSD.

In summary, the release profiles for all composites at either times (3 h, 24 h, 48 h) are different from each other as indicated by belonging to each respective individual homogeneous group.

4 Conclusions

Granular biocomposites were prepared with and without ammonium sulfate (AS) incorporation by two design strategies: *in situ* AS addition during pellet preparation (method 1), and adsorption of AS after pellet preparation (method 2). Pellets prepared according to method 1 (C1) achieved only 10% AS content, while pellets prepared according to method 2 incorporated up to twice the ammonium content (*e.g.*, CW72, CW21).

The biogenic calcium carbonate did not undergo any evident phase change, according to XRD results. Based on the release profile in water, pellets prepared according to method 1 (*in situ* incorporation) released almost 90% ammonium within the first 3 h and are unsuitable for SRF applications. Pellets prepared according to method 2 (imbibing), however, showed a release of only *ca.* 60%, C20 *ca.* 40%, CW21 *ca.* 20%, and C22 *ca.* 10% over the same time interval with a slow-release profile thereafter. Unlike the ammonium release, almost all sulfate was released within 96 h, which indicated that the granular SRF systems are not entirely suitable for slow sulfate release. This trend concurs with the Hofmeister effect and the presence of chitosan in the granule matrix, where sulfate is inferred to function as a bridging unit to the amino sites of the chitosan backbone upon sulfate binding. A statistical analysis showed that the various pellet systems showed significantly different release ($p = 0.05$) of NH_4^+ at 3 h, 24 h and 48 h.

This study demonstrates a facile synthetic route for the innovative use of biomass additives to yield granular composites with dual-functionality: (i) SRF carrier systems for AS, and (ii) a secondary role as a soil amendment material for crop production. Future studies are required to assess decomposition profiles in soil media, nutrient release and degassing of soil samples to provide a more suitable sulfate release profile that parallels the trend for ammonium. Further, plant growth studies are required to assess the NUE of these nutrient carrier systems, alongside conventional inorganic AS (without granule carrier) fertilizer.

Data availability

The data supporting this article have been included as part of the ESI.†

Author contributions

L. D. W.: funding, project supervision & editing; B. G. K. S.: writing, characterization, data analysis, synthesis, editing; N. B.: experimental, characterization, data analysis, editing; B. B.: data analysis and editing.

Conflicts of interest

There are no conflicts to declare.

Acknowledgements

LDW acknowledges the support funding provided by the Government of Canada through the Natural Sciences and Engineering Research Council of Canada (NSERC Discovery Grant Number: RGPIN 04315-2021). The Saskatchewan Structural Science Centre (SSSC) is acknowledged for providing facilities to conduct this research and scholarship support to BES. This work was carried out on Treaty 6 Territory and the Homeland of the Métis. As such, we pay our respect to the First Nations and Métis ancestors of this place and reaffirm our relationship with one another. Wayne Thiessen (Ceres Industries) is acknowledged for provision of an industrial sample of ammonium sulfate. Deysi J. Venegas-García is gratefully acknowledged for her assistance with the statistical analysis.

Notes and references

1 S. Buckingham, C. F. E. Topp, P. Smith, V. Eory, D. R. Chadwick, C. K. Baxter, J. M. Cloy, S. Connolly, E. C. Cooledge, N. J. Cowan, J. Drewer, C. Duffy, N. J. Fox, A. Jebari, B. Jenkins, D. J. Krol, K. A. Marsden, G. A. McAuliffe, S. J. Morrison, V. O'Flaherty, R. Ramsey, K. G. Richards, R. Roehe, J. Smith, K. Smith, T. Takahashi, R. E. Thorman, J. Williams, J. Wiltshire and R. M. Rees, Greenhouse Gas and Ammonia Emission Mitigation Priorities for UK Policy Targets, *Front. Agr. Sci. Eng.*, 2023, DOI: 10.15302/J-FASE-2023495.

2 G. Chataut, B. Bhatta, D. Joshi, K. Subedi and K. Kafle, Greenhouse Gases Emission from Agricultural Soil: A Review, *J. Agric. Food Res.*, 2023, **11**, 100533, DOI: 10.1016/j.jafr.2023.100533.

3 E. L. Birch, A Review of "Climate Change 2014: Impacts, Adaptation, and Vulnerability" and "Climate Change 2014: Mitigation of Climate Change", *J. Am. Plan. Assoc.*, 2014, **80**(2), 184–185, DOI: 10.1080/01944363.2014.954464.

4 Y. Yang, L. Liu, P. Liu, J. Ding, H. Xu and S. Liu, Improved Global Agricultural Crop- and Animal-Specific Ammonia Emissions during 1961–2018, *Agric., Ecosyst. Environ.*, 2023, **344**, 108289, DOI: 10.1016/j.agee.2022.108289.

5 L. Jiang, J. Yu, S. Wang, X. Wang, L. Schwark and G. Zhu, Complete Ammonia Oxidization in Agricultural Soils: High Ammonia Fertilizer Loss but Low N2O Production, *Global Change Biol.*, 2023, **29**(7), 1984–1997, DOI: 10.1111/gcb.16586.

6 Q. Duan, S. Jiang, F. Chen, Z. Li, L. Ma, Y. Song, X. Yu, Y. Chen, H. Liu and L. Yu, Fabrication, Evaluation Methodologies and Models of Slow-Release Fertilizers: A Review, *Ind. Crops Prod.*, 2023, **192**, 116075, DOI: 10.1016/j.indcrop.2022.116075.

© 2024 The Author(s). Published by the Royal Society of Chemistry

Open Access Article. Published on 27 August 2024. Downloaded on 2/20/2026 7:33:38 AM. This article is licensed under a Creative Commons Attribution-NonCommercial 3.0 Unported Licence.

7 M. M. Almutari, Synthesis and Modification of Slow-Release Fertilizers for Sustainable Agriculture and Environment: A Review, *Arabian J. Geosci.*, 2023, **16**(9), 518, DOI: 10.1007/s12517-023-11614-8.
8 Y. Xiang, Y. Liu, M. Gong, Y. Tong, Y. Liu, G. Zhao and J. Yang, Preparation of Novel Biodegradable Polymer Slow-Release Fertilizers to Improve Nutrient Release Performance and Soil Phosphorus Availability, *Polymers*, 2023, **15**(10), 2242, DOI: 10.3390/polym15102242.
9 S. Fertahi, M. Ilsouk, Y. Zeroual, A. Oukarroum and A. Barakat, Recent Trends in Organic Coating Based on Biopolymers and Biomass for Controlled and Slow Release Fertilizers, *J. Controlled Release*, 2021, **330**, 341–361, DOI: 10.1016/j.jconrel.2020.12.026.
10 D. Lawrencia, S. K. Wong, D. Y. S. Low, B. H. Goh, J. K. Goh, U. R. Ruktanonchai, A. Soottitantawat, L. H. Lee and S. Y. Tang, Controlled Release Fertilizers: A Review on Coating Materials and Mechanism of Release, *Plants*, 2021, **10**(2), 238, DOI: 10.3390/plants10020238.
11 Z. Li, Y. Zhang and Y. Li, Zeolite As Slow Release Fertilizer On Spinach Yields and Quality in a Greenhouse Test, *J. Plant Nutr.*, 2013, **36**(10), 1496–1505, DOI: 10.1080/01904167.2013.790429.
12 G. Abhiram, P. Bishop, P. Jeyakumar, M. Grafton, C. E. Davies and M. McCurdy, Formulation and Characterization of Polyester-Lignite Composite Coated Slow-Release Fertilizers, *J. Coat. Technol. Res.*, 2023, **20**(1), 307–320, DOI: 10.1007/s11998-022-00670-6.
13 A. Firmanda, F. Fahma, K. Syamsu, M. Mahardika, L. Suryanegara, A. Munif, M. Gozan, K. Wood, R. Hidayat and D. Yulia, Biopolymer-Based Slow/Controlled-Release Fertilizer (SRF/CRF): Nutrient Release Mechanism and Agricultural Sustainability, *J. Environ. Chem. Eng.*, 2024, **12**(2), 112177, DOI: 10.1016/j.jece.2024.112177.
14 H. Lü, X. Wang, Z. Pang and S. Zhao, Assessment of the Crucial Factors Influencing the Responses of Ammonia and Nitrous Oxide Emissions to Controlled Release Nitrogen Fertilizer: A Meta-Analysis, *J. Integr. Agric.*, 2023, **22**(11), 3459–3559, DOI: 10.1016/j.jia.2023.07.008.
15 C. Zhao, J. Xu, H. Bi, Y. Shang and Q. Shao, A Slow-Release Fertilizer of Urea Prepared *via* Biochar-Coating with Nano-SiO-Starch-Polyvinyl Alcohol: Formulation and Release Simulation, *Environ. Technol. Innovation*, 2023, **32**, 103264, DOI: 10.1016/j.eti.2023.103264.
16 K. Lubkowski, A. Smorowska, B. Grzmil and A. Kozłowska, Controlled-Release Fertilizer Prepared Using a Biodegradable Aliphatic Copolyester of Poly(Butylene Succinate) and Dimerized Fatty Acid, *J. Agric. Food Chem.*, 2015, **63**(10), 2597–2605, DOI: 10.1021/acs.jafc.5b00518.
17 J. Lian, W. Liu, L. Meng, J. Wu, A. Zeb, L. Cheng, Y. Lian and H. Sun, Effects of Microplastics Derived from Polymer-Coated Fertilizer on Maize Growth, Rhizosphere, and Soil Properties, *J. Cleaner Prod.*, 2021, **318**, 128571, DOI: 10.1016/j.jclepro.2021.128571.
18 M. Solgi, B. G. K. Steiger and L. D. Wilson, A Fixed-Bed Column with an Agro-Waste Biomass Composite for Controlled Separation of Sulfate from Aqueous Media, *Separations*, 2023, **10**(4), 262, DOI: 10.3390/separations10040262.
19 B. G. K. Steiger, Z. Zhou, Y. A. Anisimov, R. W. Evitts and L. D. Wilson, Valorization of Agro-Waste Biomass as Composite Adsorbents for Sustainable Wastewater Treatment, *Ind. Crops Prod.*, 2023, **191**, 115913, DOI: 10.1016/j.indcrop.2022.115913.
20 M. H. Mohamed, I. A. Udoetok, M. Solgi, B. G. K. Steiger, Z. Zhou and L. D. Wilson, Design of Sustainable Biomaterial Composite Adsorbents for Point-of-Use Removal of Lead Ions From Water, *Front. Water*, 2022, **4**, 739492, DOI: 10.3389/frwa.2022.739492.
21 I. Younes and M. Rinaudo, Chitin and Chitosan Preparation from Marine Sources. Structure, Properties and Applications, *Mar. Drugs*, 2015, **13**(3), 1133–1174, DOI: 10.3390/md13031133.
22 B. Terkula Iber, N. Azman Kasan, D. Torsabo and J. Wese Omuwa, A Review of Various Sources of Chitin and Chitosan in Nature, *J. Renewable Mater.*, 2022, **10**(4), 1097–1123, DOI: 10.32604/jrm.2022.018142.
23 K. J. Fahnestock, M. S. Austero and C. L. Schauer, Natural Polysaccharides: From Membranes to Active Food Packaging, in *Biopolymers*, Wiley Online Books; John Wiley & Sons, Inc., Hoboken, NJ, USA, 2011, pp. 59–80, DOI: 10.1002/9781118164792.ch3.
24 G. Crini, Non-Conventional Low-Cost Adsorbents for Dye Removal: A Review, *Bioresour. Technol.*, 2006, **97**(9), 1061–1085, DOI: 10.1016/j.biortech.2005.05.001.
25 *Chitosan*, ed. S. Ahmed and S. Ikram, John Wiley & Sons, Inc., Hoboken, NJ, USA, 2017, DOI: 10.1002/9781119364849.
26 Y. A. Anisimov, B. G. K. Steiger, D. E. Cree and L. D. Wilson, Moisture Content and Mechanical Properties of Bio-Waste Pellets for Fuel and/or Water Remediation Applications, *J. Compos. Sci.*, 2023, **7**(3), 100, DOI: 10.3390/jcs7030100.
27 H. Faridi and A. Arabhosseini, Application of Eggshell Wastes as Valuable and Utilizable Products: A Review, *Res. Agric. Eng.*, 2018, **64**(2), 104–114, DOI: 10.17221/6/2017-RAE.
28 J. D. Holmes, J. E. Sawyer, P. Kassel and D. R. Diaz, Using Ground Eggshells as a Liming Material in Corn and Soybean Production, *Crop Manag.*, 2011, **10**(1), 1–12, DOI: 10.1094/CM-2011-1129-01-RS.
29 M. Á. Olego, M. J. Quiroga, R. López and E. Garzón-Jimeno, The Importance of Liming with an Appropriate Liming Material: Long-Term Experience with a Typic Palexerult, *Plants*, 2021, **10**(12), 2605, DOI: 10.3390/plants10122605.
30 A. Laca, A. Laca and M. Díaz, Eggshell Waste as Catalyst: A Review, *J. Environ. Manage.*, 2017, **197**, 351–359, DOI: 10.1016/j.jenvman.2017.03.088.
31 S. Aditya, J. Stephen and M. Radhakrishnan, Utilization of Eggshell Waste in Calcium-Fortified Foods and Other Industrial Applications: A Review, *Trends Food Sci. Technol.*, 2021, **115**, 422–432, DOI: 10.1016/j.tifs.2021.06.047.
32 A. S. Ma'mor, N. H. Wahida and A. R. Nur Firdaus, The Application of Eggshell and Fruit Peels as Soil Amendment on The Growth Performance and Yield of Corn (Zea

Open Access Article. Published on 27 August 2024. Downloaded on 2/20/2026 7:33:38 AM. This article is licensed under a Creative Commons Attribution-NonCommercial 3.0 Unported Licence.

Mays L.), *IOP Conf. Ser. Earth Environ. Sci.*, 2023, **1182**(1), 012040, DOI: 10.1088/1755-1315/1182/1/012040.

33 M. Hamza, K. Farooq, Z. Rehman, H. Mujtaba and U. Khalid, Utilization of Eggshell Food Waste to Mitigate Geotechnical Vulnerabilities of Fat Clay: A Micro–Macro-Investigation, *Environ. Earth Sci.*, 2023, **82**(10), 247, DOI: 10.1007/s12665-023-10921-3.

34 J.-I. Lee, J.-M. Kim, S.-C. Yoo, E. H. Jho, C.-G. Lee and S.-J. Park, Restoring Phosphorus from Water to Soil: Using Calcined Eggshells for P Adsorption and Subsequent Application of the Adsorbent as a P Fertilizer, *Chemosphere*, 2022, **287**, 132267, DOI: 10.1016/j.chemosphere.2021.132267.

35 B. Tombarkiewicz, J. Antonkiewicz, M. W. Lis, K. Pawlak, M. Trela, R. Witkowicz and O. Gorczyca, Chemical Properties of the Coffee Grounds and Poultry Eggshells Mixture in Terms of Soil Improver, *Sci. Rep.*, 2022, **12**(1), 2592, DOI: 10.1038/s41598-022-06569-x.

36 K. Ganesan, C. Kailasanathan, M. R. Sanjay, P. Senthamaraikannan and S. S. Saravanakumar, A New Assessment on Mechanical Properties of Jute Fiber Mat with Egg Shell Powder/Nanoclay-Reinforced Polyester Matrix Composites, *J. Nat. Fibers*, 2020, **17**(4), 482–490, DOI: 10.1080/15440478.2018.1500340.

37 H. M. Baker and K. F. Alzboon, Spectrophotometric Determination of Ammonia Using Ninhydrin Assay and Kinetic Studies, *Eur. J. Chem.*, 2015, **6**(2), 135–140, DOI: 10.5155/eurjchem.6.2.135-140.1178.

38 IS 3025 (Part 24): Method of Sampling and Test (Physical and Chemical) for Water and Wastewater, Part 24: Sulphates (First Revision), 2003.

39 F. Wang, Z. Shen and A. Al-Tabbaa, An Evaluation of Stabilised/Solidified Contaminated Model Soil Using PC-Based and MgO-Based Binders under Semi-Dynamic Leaching Conditions, *Environ. Sci. Pollut. Res.*, 2018, **25**(16), 16050–16060, DOI: 10.1007/s11356-018-1591-4.

40 N. K. Kınaytürk, B. Tunalı and D. Türköz Altuğ, Eggshell as a Biomaterial Can Have a Sorption Capability on Its Surface: A Spectroscopic Research, *R. Soc. Open Sci.*, 2021, **8**(6), 210100, DOI: 10.1098/rsos.210100.

41 T. Emiola-Sadiq, L. Zhang and A. K. Dalai, Thermal and Kinetic Studies on Biomass Degradation *via* Thermogravimetric Analysis: A Combination of Model-Fitting and Model-Free Approach, *ACS Omega*, 2021, **6**(34), 22233–22247, DOI: 10.1021/acsomega.1c02937.

42 W. D. Halstead, Thermal Decomposition of Ammonium Sulphate, *J. Appl. Chem.*, 2007, **20**(4), 129–132, DOI: 10.1002/jctb.5010200408.

43 R. Kiyoura and K. Urano, Mechanism, Kinetics, and Equilibrium of Thermal Decomposition of Ammonium Sulfate, *Ind. Eng. Chem. Process Des. Dev.*, 1970, **9**(4), 489–494, DOI: 10.1021/i260036a001.

44 M. A. Rahman and T. Oomori, Structure, Crystallization and Mineral Composition of Sclerites in the Alcyonarian Coral, *J. Cryst. Growth*, 2008, **310**(15), 3528–3534, DOI: 10.1016/j.jcrysgro.2008.04.056.

45 Y. Zhang, H. Li, Y. Zhang, F. Song, X. Cao, X. Lyu, Y. Zhang and J. Crittenden, Statistical Optimization and Batch Studies on Adsorption of Phosphate Using Al-Eggshell, *Adsorpt. Sci. Technol.*, 2018, **36**(3–4), 999–1017, DOI: 10.1177/0263617417740790.

46 G. Abhiram, M. Grafton, P. Jeyakumar, P. Bishop, C. E. Davies and M. McCurdy, Iron-Rich Sand Promoted Nitrate Reduction in a Study for Testing of Lignite Based New Slow-Release Fertilisers, *Sci. Total Environ.*, 2023, **864**, 160949, DOI: 10.1016/j.scitotenv.2022.160949.

47 J. Juarros-Basterretxea, G. Aonso-Diego, Á. Postigo, P. Montes-Álvarez, Á. Menéndez-Aller and E. García-Cueto, Post-Hoc Tests in One-Way ANOVA: The Case for Normal Distribution, *Methodology*, 2024, **20**(2), 84–99, DOI: 10.5964/meth.11721.

48 C. E. Agbangba, E. Sacla Aide, H. Honfo and R. Glèlè Kakai, On the Use of Post-Hoc Tests in Environmental and Biological Sciences: A Critical Review, *Heliyon*, 2024, **10**(3), e25131, DOI: 10.1016/j.heliyon.2024.e25131.

© 2024 The Author(s). Published by the Royal Society of Chemistry